

Planar UWB MIMO-Diversity Antenna with Dual Notch Characteristics

Kamel S. Sultan* and Haythem H. Abdullah

Abstract—This paper introduces a novel MIMO UWB antenna with dual notches. The proposed antenna is based on Quasi Self Complementary (QSC) method to give wide impedance bandwidth from 2.4 GHz to more than 12 GHz. The proposed antenna consists of a semi-elliptical patch that is fed by a tapered microstrip line. The antenna is designed on an FR-4 substrate with compact size $20\text{ mm} \times 15\text{ mm} \times 1.5\text{ mm}$. The dual notched bands are achieved by using a square ring printed on the bottom of the substrate to reject WiMAX at 3.6 GHz. Also, a C-shaped slot is etched in the radiating patch to reject interference with the WLAN band at 5.8 GHz. In the proposed MIMO antenna, the isolation reduction is achieved utilizing diversity technique to minimize the mutual coupling between the antennas. The isolation between MIMO elements is more than 20 dB. The envelope correlation coefficient (ECC), diversity gain (DG), total active reflection coefficient (TARC), furthermore, channel capacity loss (CCL) are measured and calculated. The proposed antenna is designed, simulated, and measured. A good agreement is shown between the experimental and simulated results.

1. INTRODUCTION

In recent years, Multiple-Input-Multiple-Output (MIMO) have been developed to be essential in most of wireless communications systems to make best use of the multipath scattering phenomena either to increase the system capacity, to enhance the overall channel gain, or to mitigate the fading effect according to the type of channel. Furthermore, MIMO technology is used to improve reliability, excessive increase of data rates, and enhancement of capacity without exhaustion of transmitted power and bandwidth [1]. The antenna designers confront two main problems in any MIMO design; the first one is the implementation of multiple antennas in the close size of the portable devices whereas the second one is the isolation between elements to reduce mutual coupling in the proposed band. Therefore, the performance of the antenna is deteriorated with increasing the mutual coupling between the elements [2]. Since the Ultra-Wide-Band (UWB) spectrum is occupied from 3.1 GHz to 10.6 GHz according to the Federal Communication Commission (FCC), it has various applications such as medical applications, multimedia, and personal communications. In spite of several advantages of UWB systems, multipath fading is the main issue of UWB systems [3]. Therefore, MIMO technique has been combined with UWB to solve this issue. Several studies of using MIMO technology in UWB applications are reported in [4–12].

Extensive research efforts have been exerted in minimizing UWB antenna to meet the requirements of portable devices [7–15]. A Koch fractal UWB antenna with size $20 \times 15\text{ mm}^2$ is introduced in [7] to operate from 4.3 to 12 GHz. Several fractal shapes have been reported to design UWB antenna, especially hexagon-shaped antenna [8], Koch snowflake-shaped antenna [9], Sierpinski triangle antenna [8, 9], slotted interconnected ring resonator [10], and a combination of monopole and metamaterial [11]. However, in the assigned wide band of UWB applications, the MIMO

Received 12 March 2019, Accepted 22 May 2019, Scheduled 11 June 2019

* Corresponding author: Kamel S. Sultan (kamelsultan@eri.sci.eg).

The authors are with the Electronics Research Institute, Dokki, Giza, Egypt.

system that operates in UWB suffers from the electromagnetic interference in the existing narrow-band communications such as WiMAX band (3.6–3.8 GHz) and WLAN band (5.725–5.825 GHz) [12]. Therefore, several techniques have been reported to avoid interference, for instance, inserting different shapes of slots (U-shapes, T-shape, meander, C-shape) [13]. In [14], the authors introduce a UWB MIMO antenna with dual notches (WLAN and X-bands) by inserting an open slot and an SRR in the ground plane. Furthermore, the authors insert a Y-shaped slot as Defect Ground Structure (DGS) in the ground plane to reduce the mutual coupling. Yoon et al. [15] introduce heptagonal MIMO UWB antennas placed orthogonally on the same substrate to suppress the mutual coupling and insert a slot to reject WLAN band. On the other hand, for the full utilization of MIMO system, envelope correlation coefficient and mutual coupling should be minimized. Therefore, through the last years, different methods to reduce mutual coupling are introduced because of the close space between UWB antenna elements. Zhang et al. [16] introduce a planar triangular UWB antenna, and a tree-like structure is inserted on the ground plane between the two elements to achieve a wideband isolation greater than 16 dB. On the other hand, Ren et al. [17] reduce the mutual coupling between antennas by placing the antenna elements perpendicular to each other and using a narrow slot on the ground. Moreover, high isolation is achieved in [18] by inserting stubs on the ground plane and a T-shaped slot between radiators. Several other methods have been introduced, especially DGS, Electromagnetic Band Gap (EBG), reflector of T-shape, meandered line, Y-shaped stub, electrical LC resonators, and different polarizations [19–21]. Furthermore, all these MIMO techniques have large size with low isolation coefficient.

In this paper, a compact dual band-notched MIMO/diversity Quasi Self-Complementary antenna for UWB applications is presented. A very low mutual coupling is achieved between antenna elements by using diversity technique (20 dB). A MIMO/diversity QSCMA is introduced to operate from 2.4 GHz to 12 GHz. The proposed antenna consists of a semi-ellipse radiator with a C-shaped slot and a square ring to reject WLAN band and WiMAX band, respectively. The UWB antenna is designed on an FR-4 substrate with small size $20 \times 15 \text{ mm}^2$. A four elements MIMO antenna is introduced to enhance channel capacity loss ($\text{CCL} < 0.3 \text{ bit/s/Hz}$).

This paper is organized as follows. Section 2 describes the UWB antenna design and its results (simulation and measurements). Section 3 explains the MIMO antenna performance and compares between simulated and measured results. Finally, Section 4 introduces the conclusions of this research.

2. ANTENNA DESIGN

The proposed antenna consists of a semi-elliptical monopole printed on the top with counterpart semi-elliptical slot etched from the ground plane which is known as Quasi Self-Complementary technique. To achieve the miniaturization of the size and width of the band phenomena, the antenna is fed by a tapered line with a characteristic impedance 50 ohm at the feed point. The linear tapered microstrip line is added to match the input impedance of the antenna, where the input impedance of self-complementary equals 188.5Ω [11, 22]. The antenna is printed on a commercial FR-4 material substrate with dielectric constant 4.5, thickness 1.5 mm, and tangential loss 0.025. Fig. 1(a) depicts the geometry of the proposed antenna while the front and back views of the prototype are shown in Fig. 1(b) and Fig. 1(c), respectively. All dimensions are presented in Table 1. The antenna is designed using CST Microwave Studio 2017. The proposed antenna is designed to operate from 2.4 GHz to more than 12 GHz to be used in UWB applications. Fig. 2 shows the comparison between simulated and measured reflection coefficients of the proposed antenna.

Table 1. Antenna parameters (all dimensions in mm).

Parameter	R_1	R_2	L_1	L_2	L_3	W_1	W_2	W_3	W_4
Value	9	5.5	7.5	6.8	20	2.85	1.3	10	15
Parameter	L_4	L_5	L_6	L_7	S_1	L_8	L_9	S_2	d_2
Value	8	4	9.5	7.	1.5	37	46	2	0.2

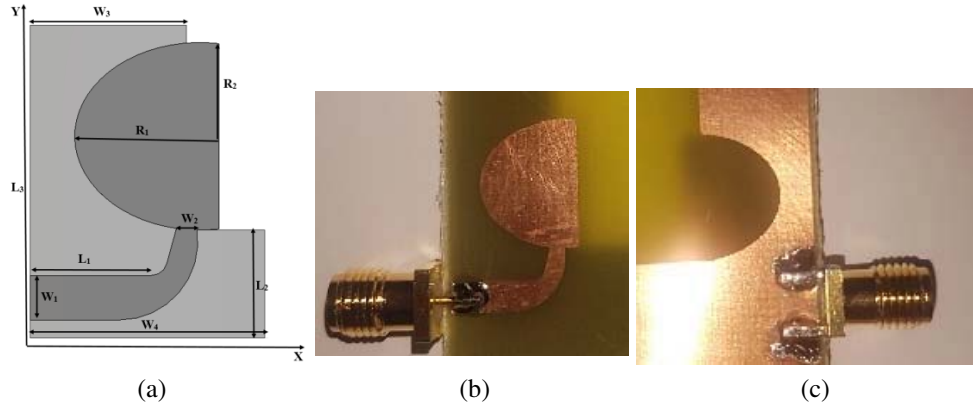


Figure 1. (a) antenna geometry. (b) Photo of front view. (c) Photo of back view.

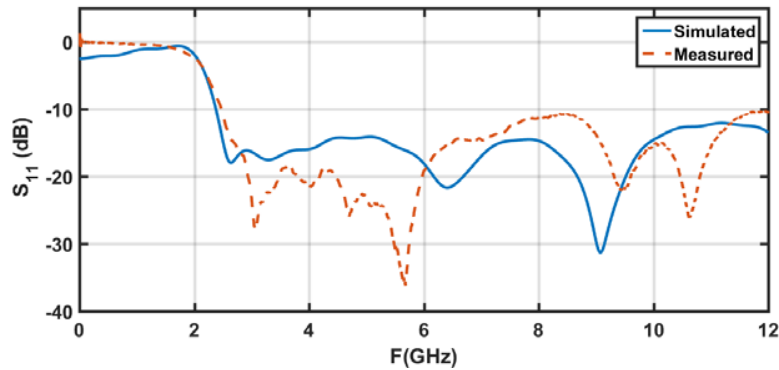


Figure 2. Reflection coefficient of UWB antenna (simulated, and measured).

In order to achieve dual band notch characteristics to suppress interference with WiMAX and WLAN bands, a square ring is printed on the bottom side of substrate, and a C-shaped slot is etched from semi-elliptical patch because they have good narrow-band rejection characteristics. Dimensions of the square ring and C-shaped slot are tuned to reject the proposed two bands according to the equations of rejected bands introduced in literature as shown in Equations (1) and (2). These two shapes, square ring and C-shaped slot, introduce notches from 3.5 GHz to 3.9 GHz and from 5.6 GHz to 6.2 GHz, respectively.

$$L_{sq} \cong \frac{c}{2f_N \sqrt{\epsilon_{eff}}} = 2(L_6 + L_7) \tag{1}$$

$$L_c \cong \frac{c}{4f_N \sqrt{\epsilon_{eff}}}, \quad L_c = 2(L_4 + L_5) - S_1 \tag{2}$$

Figure 3 shows the antenna with a dual notches (geometry and prototype). All dimensions are listed in Table 1. Fig. 4 introduces the equivalent circuit model based on lumped components for the proposed antenna with dual notches whereas the QSC antenna is expressed as two Parallel RLC sections (PRLC1 and PRLC2). The square ring strip is equivalent to a parallel LC (PLC1), and the C-shaped slot is equivalent to a parallel LC circuit (PLC2). There is a good agreement between the simulated (CST, and ADS) and measured reflection coefficients as shown in Fig. 5. To study the main parameters of the dual notches, the parametric sweep is introduced in Fig. 6 for the main parameters of notches. We note that the first notch is adjusted by the width (d_2) and length of the square ring (L_6, L_7). Furthermore, the second notch is adjusted by the width (d_2) and length (L_4, L_5) of C-shape. Fig. 7 shows the simulated and measured gains and radiation efficiencies. We can observe that the gain and efficiency drop to -1 dBi, 0.2 dBi and 35% , 50% at WiMAX and WLAN bands, respectively. The dimensions of the square ring strip and C-shaped are optimized according to Equations (1) and (2).

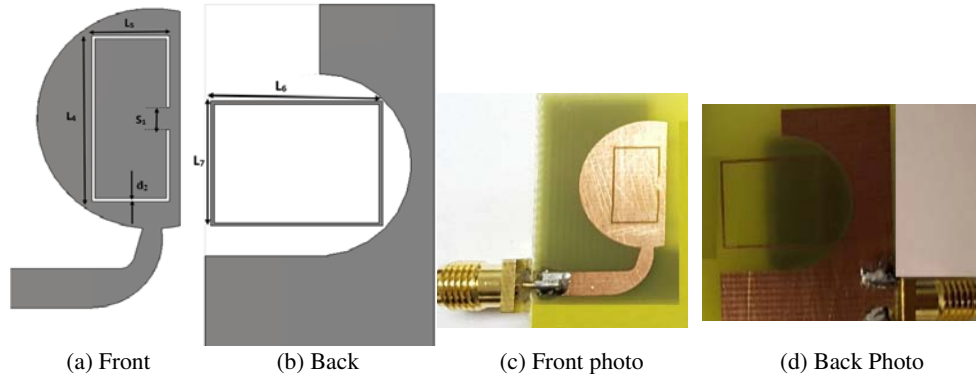


Figure 3. Geometry and photo of dual notch UWB antenna.

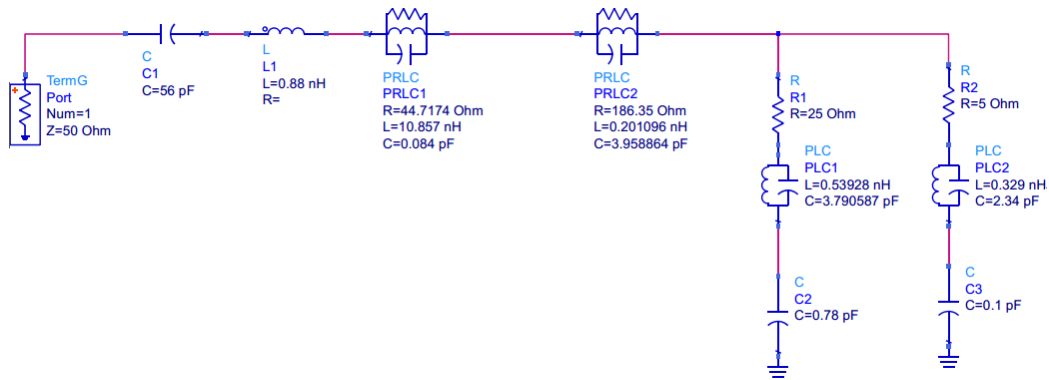


Figure 4. Equivalent circuit model for the proposed antenna.

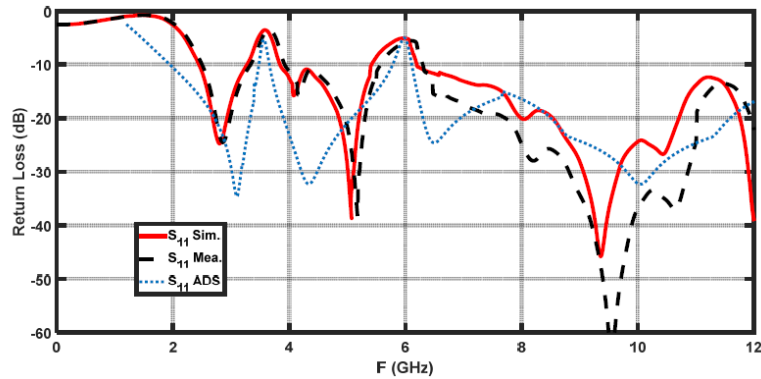


Figure 5. Reflection coefficient of antenna with a dual notch.

3. MIMO ANTENNA DESIG

3.1. MIMO Antenna Geometry

The MIMO antenna structure has 4 orthogonal elements that provide better isolation between elements without using any additional technique or decoupling circuit. The optimized geometry of the proposed 4-element UWB MIMO antenna is shown in Fig. 8. Here, the ground plane plays a significant role in the isolation performance of the proposed antenna. The diversity of the antenna positions helps to reduce coupling and achieve better isolation among them. The simulated and measured results for the

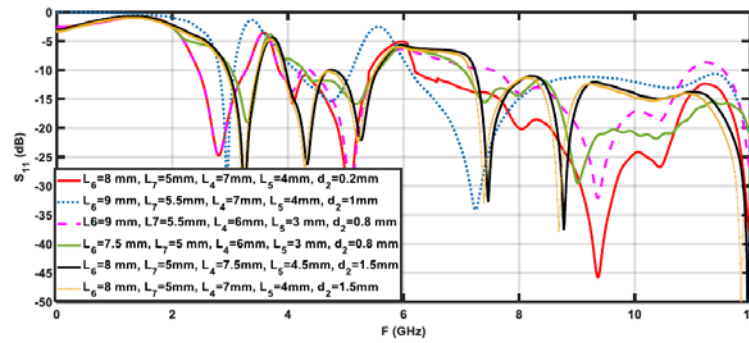


Figure 6. Simulated reflection coefficient for different values of main dual notch parameters.

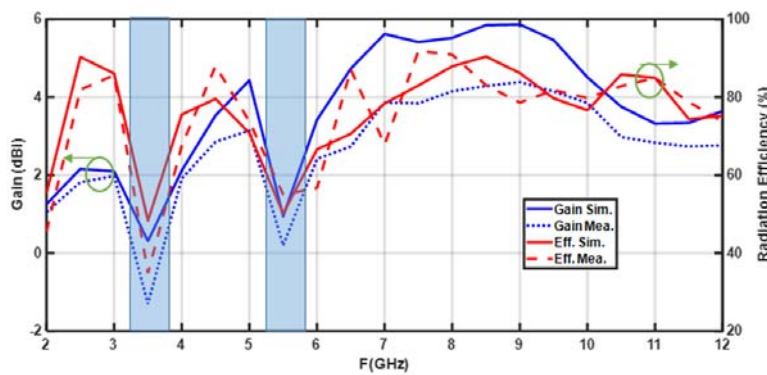


Figure 7. Simulated and measured of gain and radiation efficiency of the UWB antenna with dual notch.

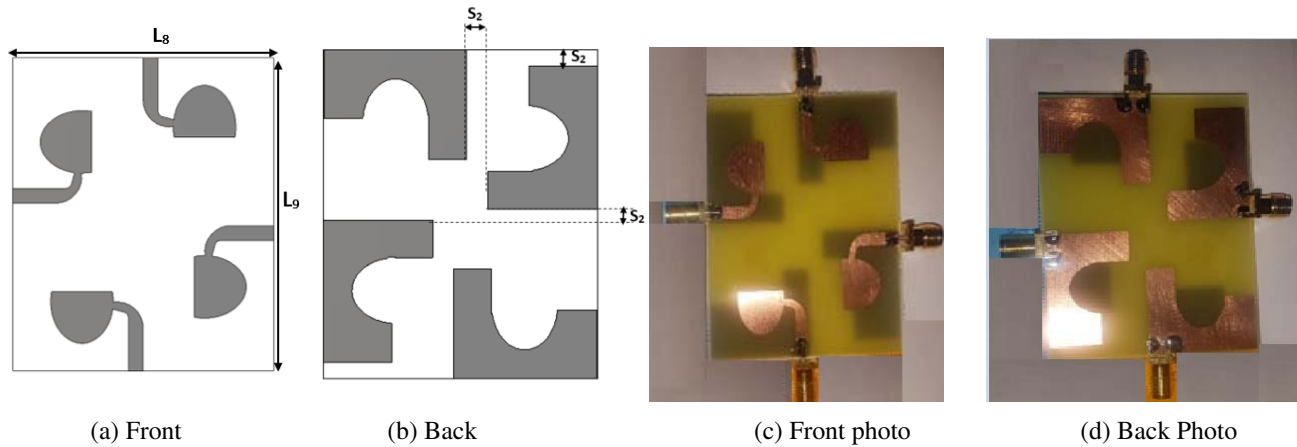


Figure 8. Geometry and photo of MIMO.

S-parameters are illustrated in Fig. 9. In this figure, only S_{11} , S_{21} , S_{31} , and S_{41} are discussed because of the symmetrical arrangement of antenna elements in the structure. A good agreement between the simulated and measured *S*-parameters is noticed. Furthermore, the dual-notch UWB-MIMO antenna is fabricated where its *S*-parameters are shown in Fig. 10 and Fig. 11, respectively.

The square ring is used to reduce the mutual coupling between antenna elements; furthermore, it is essentially used to reject WiMAX band. Fig. 12 illustrates the comparison between the simulated and measured radiation patterns for both the co- and cross-polarizations. It is noticed that the cross-

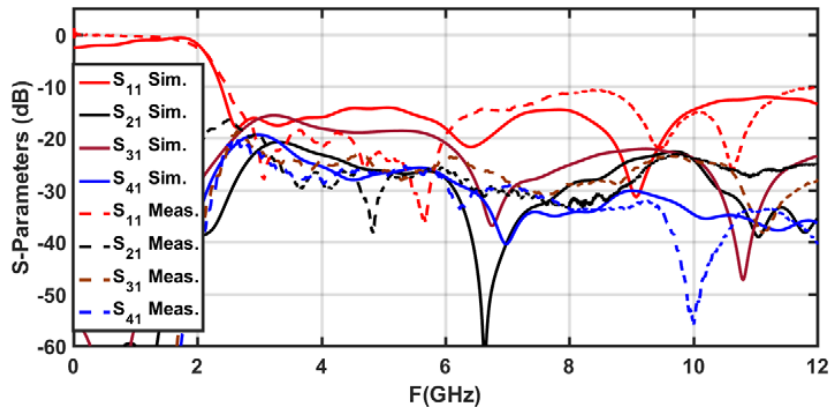


Figure 9. *S*-parameters of MIMO antenna.

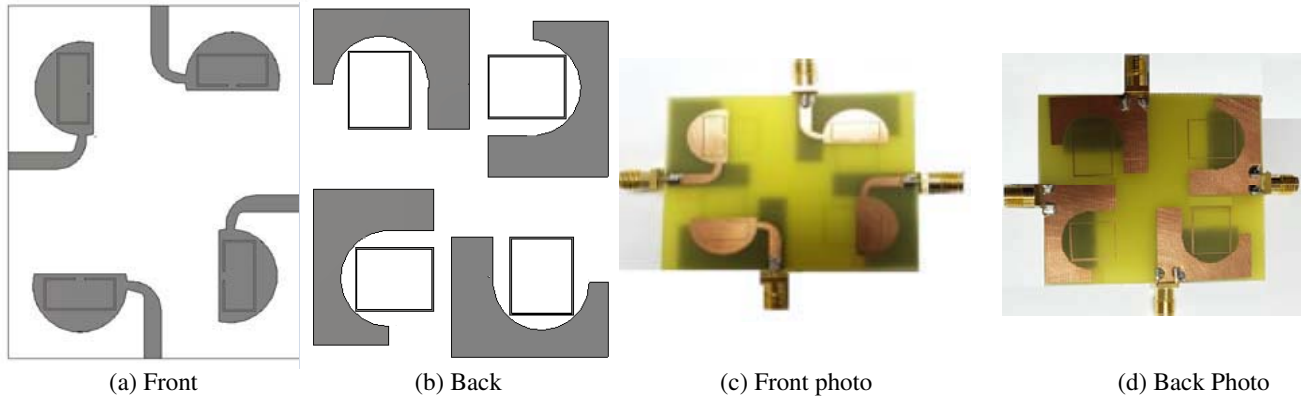


Figure 10. Geometry and photo of MIMO with notch.

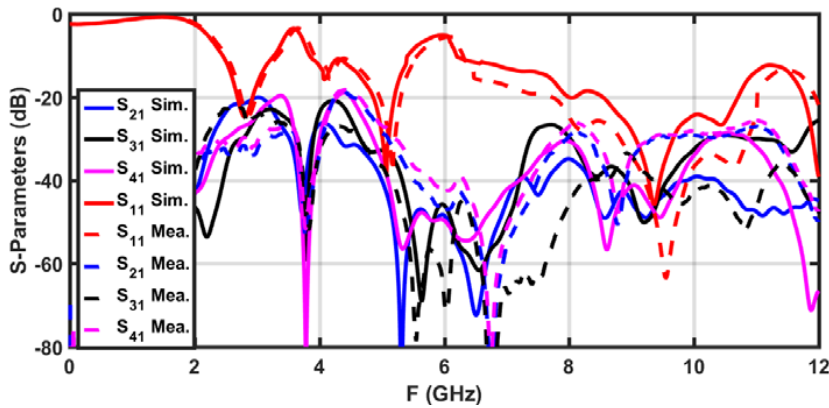


Figure 11. *S*-parameters of MIMO with dual notch (simulated, and measured).

polarized wave is negligible compared to the co-polarized wave. This indicates that the antenna is considered a linearly polarized antenna. Also, the figure indicates that the antenna behaves approximately as omnidirectional radiators.

Due to different orientations of the antennas constituting the MIMO system, the maximum direction of radiation for each element is different as shown in Fig. 13.

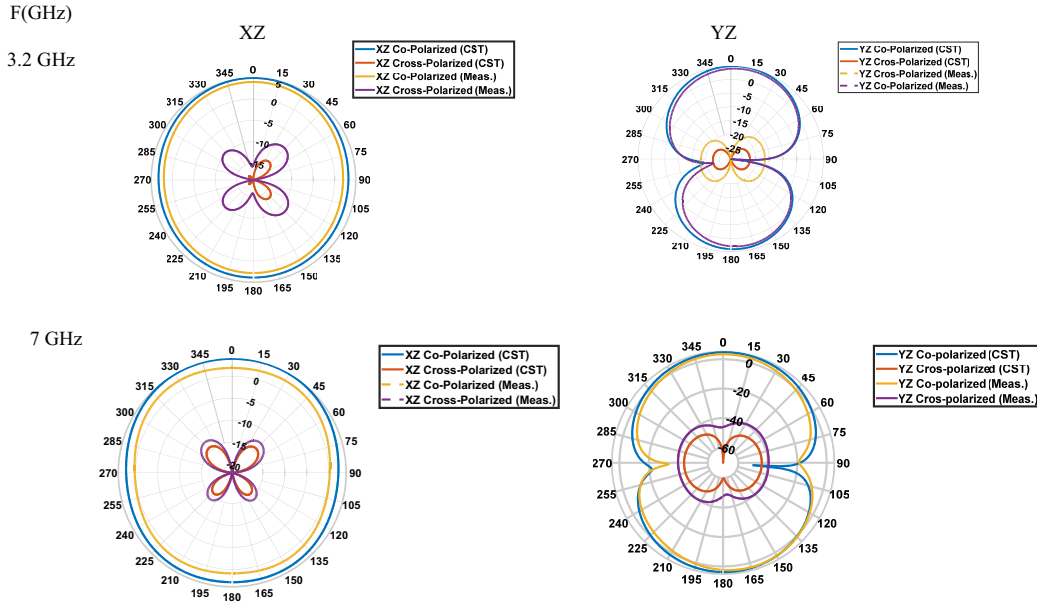


Figure 12. Simulated and measured radiation pattern of one element.

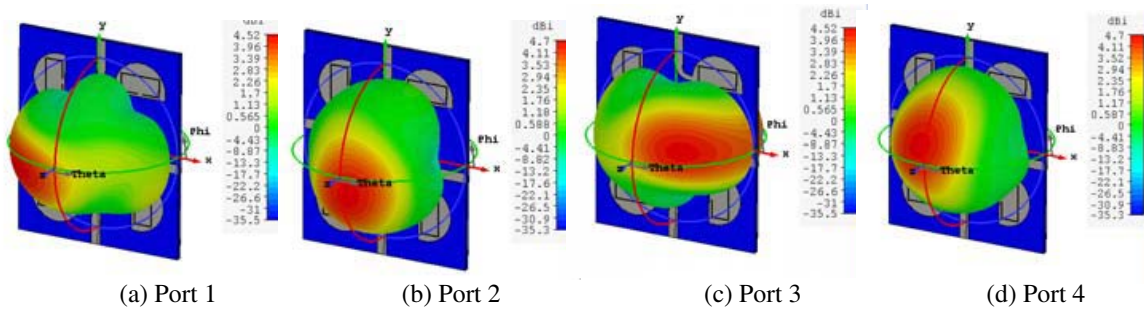


Figure 13. 3D Radiation pattern for MIMO.

3.2. MIMO Parameters

MIMO have four different parameters which should be tested to ensure that the MIMO give good performance: ECC is one of the main parameters that are used to characterize the performance of MIMO antenna. It measures the similarity between the performances of the antennas from radiation pattern point of view. The ECC can be calculated from the following form [21]

$$\rho_{nm} = \frac{|S_{nn}^* S_{nm} + S_{mn}^* S_{mm}|^2}{\left(1 - (|S_{nn}|^2 + |S_{mn}|^2)\right) \left(1 - (|S_{mm}|^2 + |S_{nm}|^2)\right)} \quad (3)$$

The value of ECC should be less than 0.5 over the operating band according to the published standard [4, 5]. Lower values of ECC mean that the two antennas are well isolated. Fig. 14(a) shows the ECC between MIMO elements. It is obvious from the figure that the ECC is less than 0.02 within the operating band. The second parameter is diversity gain (DG), which can be expressed as [21]

$$DG = 10\sqrt{1 - ECC^2} \quad (4)$$

As shown in Fig. 14(b), the DG has high values in the operating band. The total active reflection coefficient (TARC) is the third parameter that indicates the coupling between ports. Its minimum value is 0 which means that all incident power is radiated, whereas the maximum value is 1 which

means that all the incident power is reflected. The TARC greatly affects the operating bandwidth of the MIMO antenna system [21]. The TARC is calculated according to the following equation

$$\Gamma_a^t = \frac{\sqrt{\sum_{i=1}^N |b_r|^2}}{\sqrt{\sum_{i=1}^N |a_i|^2}} \quad (5)$$

$$[b] = [s][a] \quad (6)$$

where a_i and b_r are the incident signals and reflected signals, respectively. $[S]$, $[a]$, and $[b]$ represent scattering matrix, excitation vector, and scattered vector of the antenna, respectively.

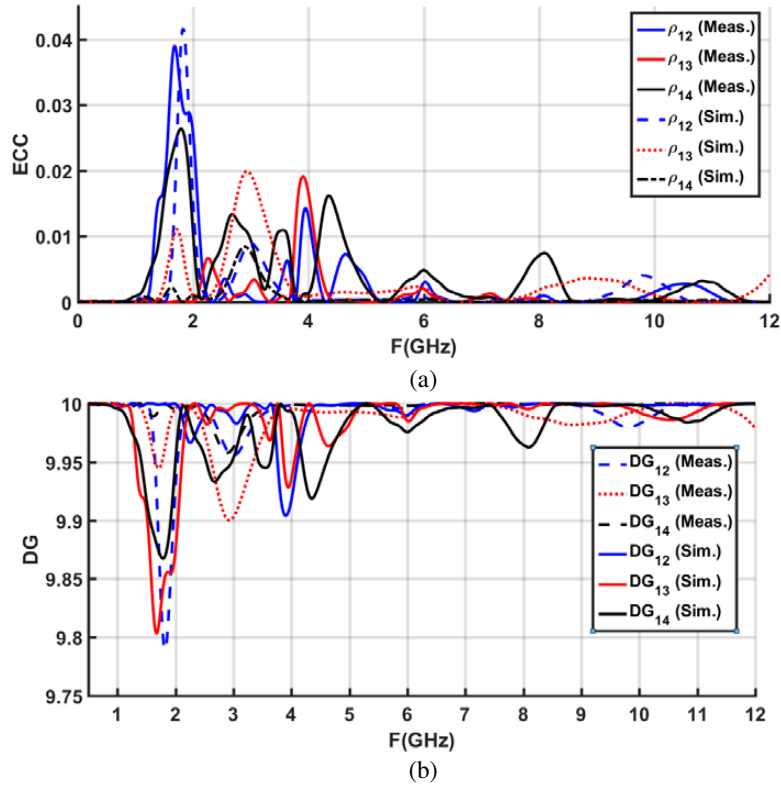


Figure 14. MIMO performance, (a) ECC, (b) DG.

Figure 15 shows the TARC curves upon exciting port one at $1e^{j0}$ when other ports have the same amplitude but different excitations phases. Some of the possible cases are introduced as shown in the figure. The values of TARC refer to the effective BW of MIMO system. We can observe that the operating BW of the proposed antenna is slightly affected by different excitation phases of the other ports. The final parameter is channel capacity loss (CCL). The standard of CLL is $CCL < 0.4$ b/s/Hz [4]. The capacity of MIMO system grows with the increase of antenna number

$$CCL = -\log_2 \det(\psi^R) \quad (7)$$

$$\psi^R = \begin{bmatrix} \rho_{11} & \rho_{12} & \rho_{13} & \rho_{14} \\ \rho_{21} & \rho_{22} & \rho_{23} & \rho_{24} \\ \rho_{31} & \rho_{32} & \rho_{33} & \rho_{34} \\ \rho_{41} & \rho_{42} & \rho_{43} & \rho_{44} \end{bmatrix}, \quad \rho_{mm} = 1 - \left| \sum_{n=1}^4 S_{mn}^* S_{nm} \right|, \quad \rho_{mp} = - \left| \sum_{n=1}^4 S_{mn}^* S_{np} \right|, \quad \text{for } m, p = 1, 2, 3 \text{ or } 4 \quad (8)$$

Figure 16 shows the simulation and the measurement of the CLL for MIMO antenna in both cases of presence or absence of the notch. The measured and simulated values of CLL are less than 0.3 bits/s/Hz through operating band except the dual notches. Additionally, the proposed MIMO antenna is compared to the previously published works shown in Table 2.

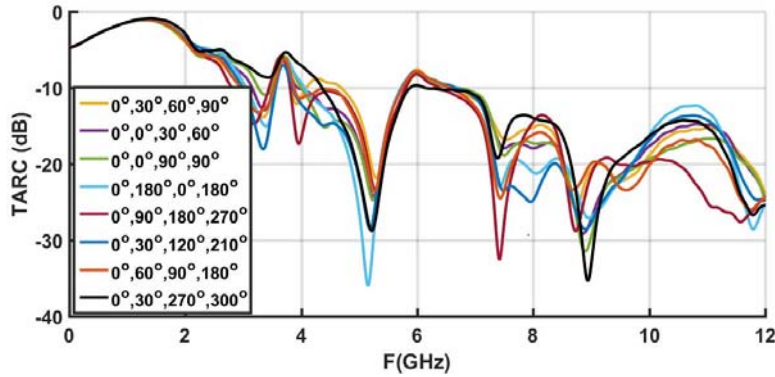


Figure 15. TARC for different cases of MIMO excitation.

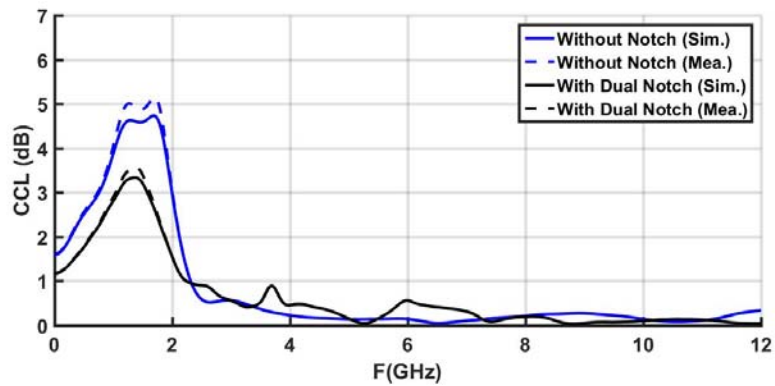


Figure 16. Channel capacity loss of MIMO.

Table 2. Comparison of this work with the previous published papers.

Ref.	No. of Ports	Size (mm ²)	BW (GHz)	No. of Notches	Gain (dBi)	Eff. (%)	ECC	DG (dB)	CCL	Isolation	Isolation technique	Dielectric Constant
[5]	2	48×48	2.5–12	1	3	90	0.005	-	-	15	Stubs	4.4
[4]	4	45×45	2–10.6	1	3.5	-	0.005	-	0.3	17	Orthogonal	4.4
[6]	4	60×60	2.7–10.6	1	3.5	-	0.063	-	-	15	BSF	4.4
[18]	4	48×48	3–11	0	3	80	-	10	-	17	Stubs/slots	4.4
[23]	4	100×100	3.1–10.6	2	-	-	0.1	-	0.3	20	Space	4.4
[24]	4	50×39.8	2.7–12	1	4.5	-	-	-	-	17	Stub/orthogonal	4.5
[25]	4	32×36 ×36 (mm ³)	3.1–10.6	0	-	60	0.0025	-	0.2	20	3-D shape	4.4
[26]	2	22×26	3.1–11.8	2	4.8	85	0.03	-	-	20	slots	4.4
[27]	2	26×40	2.2–11.4	1	5	90	0.008	-	-	20	Ground strip	4.4
This work	4	37×46	2.5–12	2	4	80	0.005	9.96	0.3	20	Orthogonal	4.5

4. CONCLUSION

A compact printed diversity MIMO UWB antenna with dual rejected bands is presented in this paper. The antenna is designed based on QSC technique to produce wide band. Four elements are introduced with overall size $37 \times 46 \text{ mm}^2$. All the prototypes introduce good impedance matching and good isolation over the range from 2.5 GHz to 12 GHz. ECC, CCL, DG, and TARC are introduced to investigate that the proposed antenna has good performance over the proposed band.

REFERENCES

1. Kaoser, T., F. Zheng, and E. Dimitrov, "An overview of ultrawide-band systems with MIMO," *Proceedings of the IEEE*, Vol. 97, No. 2, 285–312, 2009.
2. Anitha, R., P. V. Vinesh, K. C. Prakash, P. Mohanan, and K. Vasudevan, "A compact quad element slotted ground wideband antenna for MIMO applications," *IEEE Transactions on Antennas and Propagation*, Vol. 64, No. 10, 4550–4553, 2016.
3. Federal Communications Commission, Federal Communications Commission revision of part 15 of the commission's rules regarding ultra-wideband transmission system from 3.1 to 10.6 GHz, ET-Docket, Washington, DC, USA, 2002.
4. Tripathi, S., A. Mohan, and S. Yadav, "A Compact koch fractal UWB MIMO antenna with WLAN band-rejection," *IEEE Antennas and Wireless Propagation Letter*, Vol. 14, 1565–1568, March 2015.
5. Gao, P., S. He, Z. Xu, and Y. Zheng, "Compact printed UWB diversity slot antenna with 5.5-GHz band-notched characteristics," *IEEE Antenna and Wireless Propagation Letters*, Vol. 13, 376–379, 2014.
6. Kiem, N. K., H. N. B. Phuong, and D. N. Chien, "Design of compact 4×4 UWB-MIMO antenna with WLAN band rejection," *International Journal of Antennas and Propag.*, ArticleID 539094, 11 pages, 2014.
7. Li, D., F. S. Zhang, Z. N. Zhao, L. T. Ma, and X. N. Li, "UWB antenna design using patch antenna with Koch fractal boundary," *IEEE, Microwave and Millimeter Wave Technology Conf.*, Vol. 3, 1–3, 2012.
8. Werner, D. H., R. L. Haupt, and P. L. Werner, "Fractal antenna engineering: The theory and design of fractal antenna arrays," *IEEE Antennas and Propagation Magazine*, Vol. 41, No. 5, 37–58, Oct. 1999.
9. Anguera, J., C. Puente, V. Borja, and J. Soler, "Fractal-shaped antennas: A review," *Wiley Encyclopedia of RF and Microwave Engineering*, Vol. 2, 1620–1635, 2005.
10. Desai, A., T. Upadhyaya, M. Palandoken, and C. Gocen, "Dual band transparent antenna for wireless MIMO system applications," *Microwave And Optical Technology Letters*, 1–12, Feb. 2019, doi.org/10.1002/mop.31825.
11. Saraswat, R. K. and M. Kumar, "Miniaturized slotted ground UWB antenna loaded with metamaterial for WLAN and WiMAX applications," *Progress In Electromagnetics Research B*, Vol. 65, 65–80, 2016.
12. Sibal, D., M. P. Abegaonkar, and S. K. Koul, "Compact band-notched UWB antenna for MIMO applications in portable wireless devices," *Microw. Opt. Technol. Lett.*, Vol. 58, No. 6, 1390–1394, Jun. 2016.
13. Ibrahim, A. A., M. A. Abdalla, and A. Boutejdar, "A printed compact band-notched antenna using octagonal radiating patch and meander slot technique for UWB applications," *Progress In Electromagnetics Research M*, Vol. 54, 153–162, 2017.
14. Peng, L., J. Y. Xie, X. Jiang, and S. M. Li, "Investigation on ring/split-ring loaded bow-tie antenna for compactness and notched-band," *Frequenz*, Vol. 70, No. 3–4, 89–99, 2016.
15. Yoon, H. K., Y. J. Yoon, H. Kim, and C.-H. Lee, "Flexible ultra-wideband polarisation diversity antenna with band-notch function," *IET Microwaves, Antennas & Propagation*, Vol. 5, No. 12, 1463–1470, 2011.

16. Zhang, S., Z. Ying, J. Xiong, and S. He, "Ultra wide band MIMO/diversity antennas with a tree-like structure to enhance wideband isolation," *IEEE Antenna and Wireless Propagation Letters*, Vol. 8, 1279–1282, 2009.
17. Ren, J., W. Hu, Y. Yin, and R. Fan, "Compact printed MIMO antenna for UWB applications," *IEEE Antenna and Wireless Propagation Letters*, Vol. 13, 1517–1520, 2014.
18. Mao, C. X. and Q. X. Xhu, "Compact coradiator UWB/MIMO antenna with dual polarization," *IEEE Trans. Antennas Propag.*, Vol. 62, No. 9, 4474–4480, Sep. 2014.
19. Zhang, J.-Y., F. Zhang, W.-P. Tian, and Y.-L. Luo, "ACS-fed UWB MIMO antenna with shared radiator," *Electronics Letters*, Vol. 51, No. 7, 1301–1302, 2015.
20. Kumar, J., "Compact MIMO antenna," *Microwave and Optical Technology Letters*, Vol. 58, No. 6, 1294–1298, 2016.
21. Chandel, R., A. K. Gautam, and K. Rambabu, "Tapered fed compact UWB MIMO-diversity antenna with dual band-notched characteristics," *IEEE Trans. on Antennas and Propag.*, Vol. 66, No. 4, April 2018.
22. Sultan, K. S., O. M. Dardeer, and H. A. Mohamed, "Design of compact dual notched self-complementary UWB antenna," *Open Journal of Antennas and Propagation*, Vol. 5, 99–109, 2017.
23. Shehata, M., M. S. Said, and H. Mostafa "Dual notched band quad-element MIMO antenna with multitone interference suppression for IR-UWB wireless applications," *IEEE Transactions on Antennas and Propagation*, Vol. 66, No. 11, 5737–5746, November 2018.
24. Khan, A. M. S., D. Capobianco, S. Asif, A. Iftikhar, B. Ijaz, and B. D. Braaten, "Compact 4×4 UWB-MIMO antenna with WLAN band-rejected operation," *Electron Lett.*, Vol. 51, No. 14, 1048–1050, 2015.
25. Bilal, M., R. Saleem, H. H. Abbasi, M. F. Shafique, and A. K. Brown, "An FSS-based nonplanar quad-element UWB-MIMO antenna system," *IEEE Antennas Wireless Propag. Lett.*, Vol. 16, 987–990, 2017.
26. Jetti, C. R. and V. R. Nandanavanam, "Compact MIMO antenna with WLAN band notch characteristics for portable UWB systems," *Progress In Electromagnetics Research C*, Vol. 88, 1–12, 2018.
27. Jetti, C. R. and V. R. Nandanavanam, "Trident-shape strip loaded dual band-notched UWB MIMO antenna for portable device applications," *AEU-International Journal of Electronics and Communications*, Vol. 83, 11–21, 2018.